Skull Stripping in MR Images Using an Adaptive Deformable Model with Dynamic Brain Intensity Detection

Yu-Sheng Chen and Herng-Hua Chang
Computational Biomedical Engineering Laboratory (CBEL)/Department of Engineering Science and Ocean Engineering/National Taiwan University, Daan 10617 Taipei, Taiwan
Email: phil0814@gmail.com, herbertchang@ntu.edu.tw

***Abstract*—Skull stripping is an important preprocessing step in many medical image applications. Deformable models are powerful as they provide robust abilities to deform contours under the guidance of geometric properties. In particular, the charged fluid model has been shown its superiority over many existing deformable models. This paper is in an attempt to propose a new skull stripping algorithm based on the charged fluid model. To improve the segmentation accuracy, a new image balancing coefficient of using the local intensity difference along the normal line of the evolving curve is introduced. Stimulated by the concept of the Mumford-Shah model, the other balancing coefficient obtained from a global intensity difference between the interior and exterior of the evolving contour is also introduced to automate the segmentation process. We have adopted the BrainWeb and internet brain segmentation repository (IBSR) image datasets to evaluate this new algorithm. Experimental results indicated that our method produced high segmentation accuracy across a wide variety of brain magnetic resonance (MR) images, which is promising in many MR image processing applications.**

***Index Terms*—segmentation, MRI, charged fluid model, deformable model, skull stripping**

I. Introduction

Skull stripping is an important preprocessing step in many research and clinical applications. It aims to remove non-brain tissues (e.g., skull, scalp, and dura) and retain brain parenchyma in MR images. Skull-stripping brain MR images has been challenging due to the complexity of human brain structure in both health and disease across a large number of subjects. Nevertheless, many researchers have proposed different methods worldwide.

One famous approach is the brain surface extractor (BSE), which is developed based on the combination of edge detectors and morphological operators [1]. In their approach, a Marr Hildreth edge detector is first used to identify anatomical boundaries, followed by a sequence of morphological operators to separate connected tissues into individual component regions. Finally, the brain tissue is extracted based on the largest central connected component.

Manuscript received January 2, 2015; revised March 2, 2015.

Deformable models apply physical and image forces to push and pull the contour toward an object's boundary. Parametric active contours, also known as snakes, are one of the well-known deformable models proposed by Kass *et al*. [2]. Brain extraction tool (BET) is one of the successful implementations of snakes [3]. A set of parameters, including morphological and image-based forces, are applied in the tangential and normal directions of the interface to guide the evolution. However, edge-based deformable models are usually prone to noise influence and low contrast problems and are sensitive to initial contour settings.

The charged fluid model (CFM) [4] has been shown less critical than many existing deformable models in segmenting objects with sharp corners and cusps. This paper is in an attempt to propose a new brain extraction algorithm based on the charged fluid model. The ultimate goal is to establish a more robust brain extraction algorithm that overcomes disadvantages of many existing methods.

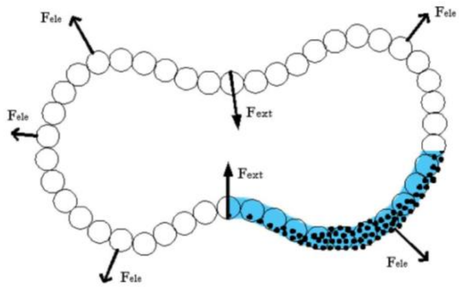

Figure 1. Charged fluid model.

II. Adaptive Deformable Model

A. Review of Charged Fluid Model

As shown in Fig. 1, the CFM is based upon the theory of electrostatics rather than that of curve evolution and geometric flows for image segmentation. The fluid elements are connected to one another by 4-connectivity when they advance. The charged fluid, behaving like a liquid, can be influenced by internal electric forces of repulsion as well as external forces from the image data.

Suppose that the charge distribution of an electrostatic system is known, the electric potential Φ can be calculated through Poisson's equation as

$$\nabla^2\Phi(\mathrm{r}) = -4\pi\rho(\mathrm{r}) \tag{1}$$

where $\rho(\mathrm{r})$ is the charge density. The corresponding electric field **E** can then be computed in terms of the scalar potential using

$$\mathrm{E}(\mathrm{r}) = -\nabla\Phi(\mathrm{r}) \tag{2}$$

To handle the problems of using multiple charged fluids, the electric potential for each charged fluid is normalized through Poisson's equation as

$$\hat{\Phi}^j_{\mathrm{ele}} = \frac{\Phi^j_{\mathrm{ele}}}{\overline{\Phi}^j}\Phi_0 \tag{3}$$

where $\hat{\Phi}^j_{\mathbf{ele}}$ is the normalized electric potential for the charged fluid *j*, $\overline{\Phi}^j$ is the mean electric potential in the charged fluid *j*, and Φ_0 is an arbitrary positive constant. The corresponding normalized charge density is then defined as

$$\hat{\rho}^j = \frac{\rho^j}{\overline{\Phi}^j}\Phi_0 \tag{4}$$

Therefore, the overall system is governed by the modified Poisson's equation

$$\nabla^2\hat{\Phi}_{\mathrm{ele}} = \nabla^2\sum_j\hat{\Phi}^j_{\mathrm{ele}} = -4\pi\sum_j\hat{\rho}^j = -4\pi\hat{\rho} \tag{5}$$

where $\hat{\Phi}_{\mathrm{ele}}$ is the normalized electric potential and $\hat{\rho}$ is the normalized charge density of the overall system at each time step. Finally, the electric field $\mathbf{E}_{\mathrm{ele}}$ is directly computed using the normalized electric potential

$$\mathrm{E}_{\mathrm{ele}} = -\nabla\hat{\Phi}_{\mathrm{ele}} \tag{6}$$

To interact with the image data, the image gradient potential is defined as

$$\Phi_{\mathrm{img}}(m,n) = \frac{|\nabla G_\sigma(m,n)\times I(m,n)|}{|\nabla G_\sigma \times I|_{\max}}\Phi_0 \tag{7}$$

where $|\cdot|$ is the modulus of the smoothed image gradients and $|\cdot|_{\max}$ is the maximum modulus in the computation domain. The corresponding image field $\mathbf{E}_{\mathrm{img}}$ is defined as

$$\mathrm{E}_{\mathrm{img}} = \nabla\Phi_{\mathrm{img}} \tag{8}$$

B. Improvement of Charged Fluid Model

To improve the brain extraction accuracy, two new different image forces are introduced. Stimulated by the concept of the Mumford-Shah model [5], we first define a new coefficient α as

$$\alpha = [I(x,y)-c_1]+[I(x,y)-c_2] \tag{9}$$

where $I(x, y)$ is the image intensity of the fluid element at (x, y), C_1 and C_2, depending on the curve, are the averages of inside the curve and respectively outside the curve using

$$\begin{cases} c_1 = \text{average}(I) \text{ inside curve} \\ c_2 = \text{average}(I) \text{ outside curve} \end{cases} \tag{10}$$

To attract the contour to the brain surface and to stop the contour from leaking through the boundary, a brain texture force is defined as [3]:

$$F_{\mathrm{img}} = \frac{2(I_{\min} - h_1)}{I_{\max} - h_{2\%}} \tag{11}$$

where $h_{2\%}$ is the intensity threshold separating the lower 2% of the cumulative histogram and h_1 is the threshold separating the intensity of skull from the local maximum intensity $I_{\max}$ using

$$h_1 = (I_{\max} - h_{2\%})T_h + h_{2\%} \tag{12}$$

where T_{h} is a constant equal to 0.5. In (11), $I_{\max}$ and $I_{\min}$ are defined as

$$I_{\min} = \mathrm{MAX}(h_{2\%}, \mathrm{MIN}(h_M, I(0), I(1), \cdots, I(d_1))) \tag{13}$$

$$I_{\max} = \mathrm{MIN}(h_{98\%}, \mathrm{MAX}(h_M, I(0), I(1), \cdots, I(d_2))) \tag{14}$$

where $h_{\underline{M}}$ is the median intensity calculated in the brain region within the contour and $I(n)$ is the intensity of a pixel on the line *n* pixels away from the origin. More specifically, $I_{\min}$ and $I_{\max}$ are the local minimum and maximum intensities of pixels on a line that starts from the contour and points inward to the brain in the normal direction; and d_1 and d_2 are the lengths of the line used to find $I_{\min}$ and $I_{\max}$, respectively. Finally, we incorporate these two new coefficients into the governing equation to create a new effective field as

$$\mathrm{E}_{\mathrm{eff}} = \alpha\cdot\mathrm{E}_{\mathrm{ele}} + \beta\cdot F_{\mathrm{img}}\cdot\mathrm{E}_{\mathrm{img}} \tag{15}$$

where β is a weighting factor for balancing between the electric and image fields.

C. Slice-by-Slice Segmentation

As shown in Fig. 2, the proposed adaptive skull stripping algorithm consists of five major phases. First, compute the smoothed images using the Gaussian filter for the entire volume. Then, place the initial contour around the center slice to start the segmentation process. In the charge distribution procedure, the electric field is computed when an electrostatic equilibrium is achieved.

Before the front deformation procedure, the system automatically computes the coefficients in (9) and (11) to advance the contour toward the brain boundaries using (15). These procedures are repeated until the entire volume is segmented.

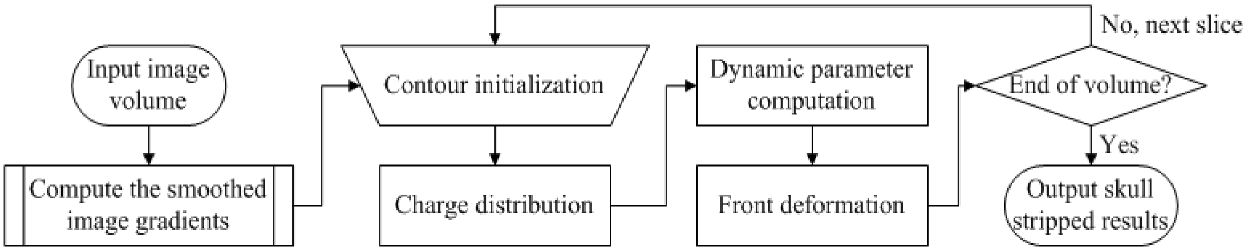

Figure 2. Flowchart of the adaptive skull stripping algorithm.

TABLE I. PERFORMANCES EVALUATION ON THE BRAINWEB IMAGE DATASETS USING THREE DIFFERENT COEFFICIENTS: CONFORMITY (K_C), SENSITIVITY (K_{St}) AND SENSIBILITY (K_{Sb})

	K_C (%)	K_{St} (%)	K_{Sb} (%)
Pn 1	97.30	98.52	98.81
Pn 3	97.30	98.56	98.77
Pn 5	97.10	98.37	98.77
Pn 7	97.12	98.44	98.72
Pn 9	97.10	T98.53	98.60
Avg. ±Std.	97.18±0.09	98.48±0.06	98.73±0.07

III. EXPERIMENTAL RESULTS

We have adopted the BrainWeb: Simulated Brain Database (SBD) [6] image data of T1-weighted MR image volumes with various levels of noise and the internet brain segmentation repository (IBSR) datasets [7]. Three different performance measure coefficients were used to evaluate the proposed algorithm [8]:

Conformity: $$K_C = 1 - \left(\frac{F_P + F_N}{T_P}\right) \times 100\% \quad (16)$$

Sensitivity: $$K_{St} = \frac{T_P}{T_P + F_N} \times 100\% \quad (17)$$

Sensibility: $$K_{Sb} = 1 - \left(\frac{F_P}{T_P + F_N}\right) \times 100\% \quad (18)$$

where T_P represents true positives, T_N true negatives, F_P false positives, F_N false negatives of the segmentation union. All coefficients have a maximum score of 100% and the higher the better.

Fig. 3 shows representative images of the BrainWeb: SBD data with different noise levels. The corresponding segmentation results are shown in Fig. 4. Table I presents the performance evaluation results of segmented images with various noise levels from 1% to 9% in the BrainWeb datasets. Each dataset consists of 60 sequential slices with 3mm slice thickness. Obviously, all evaluation coefficients were pretty high and consistently close to 100% regardless of different noise levels. Representative segmentation results on the IBSR datasets are shown in Fig. 5, where the contours were precisely located on the brain surfaces on each slice.

IV. CONCLUSIONS

We have introduced a new skull stripping algorithm based on an improved charged fluid model. To adapt the complexity of the brain structure, two new balancing coefficients were introduced and incorporated into the governing equation. A wide variety of brain MR images from the BrainWeb and the IBSR datasets were used to evaluate the proposed framework. Experimental results indicated that our method successfully stopped the leakage comparing to the traditional charged fluid model and produced high segmentation accuracy across a number of MR image volumes. We believe that this new skull stripping algorithm is promising in providing accurate segmentation results in a wide variety of MR image processing applications.

ACKNOWLEDGMENT

This work was supported by the National Science Council under Research Grant No. NSC100-2320-B-002-073-MY3.

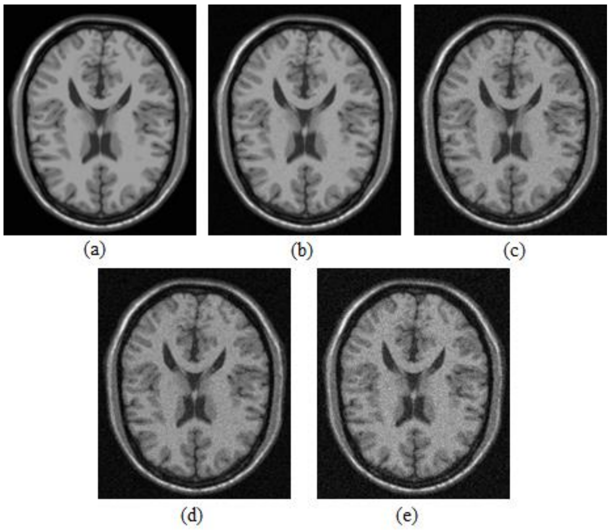

Figure 3. Original images of the BrainWeb: SBD datasets. Noise level: (a) 1%; (b) 3%; (c) 5%; (d) 7%. (e) 9%.

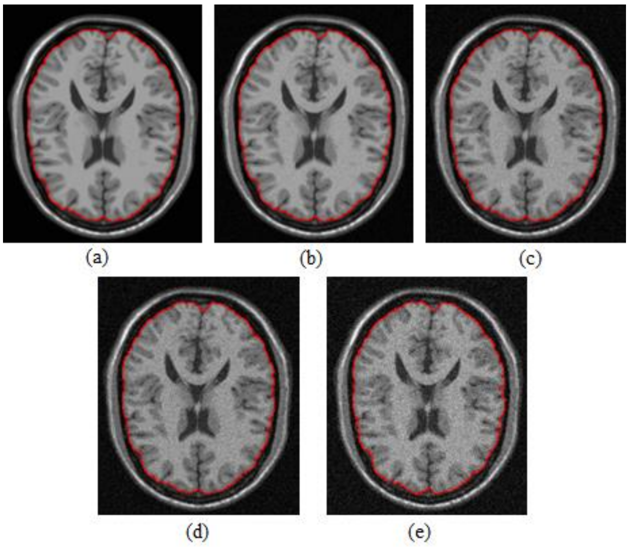

Figure 4. Visual segmentation results of the BrainWeb: SBD datasets in Fig. 3. Noise level: (a) 1%; (b) 3%; (c) 5%; (d) 7%; (e) 9%.

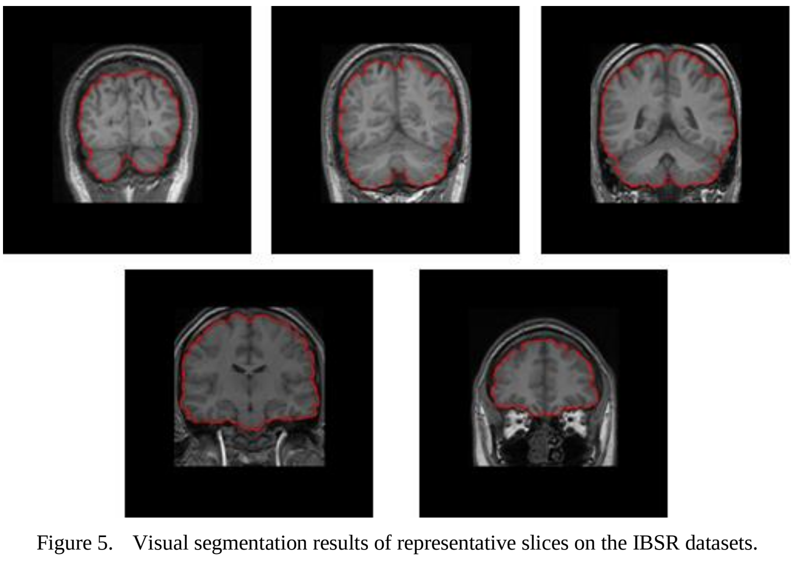

Figure 5. Visual segmentation results of representative slices on the IBSR datasets.

REFERENCES

[1] D. W. Shattuck, S. R. Sandor-Leahy, K. A. Schaper, D. A. Rottenberg, and R. M. Leahy, “Magnetic resonance image tissue classification using a partial volume model,” *NeuroImage*, vol. 13, no. 5, pp. 856-876, 2001.

[2] M. Kass, A. Witkin, and D. Terzopoulos, “Snakes: Active contourmodels,” *Int. J. Comput. Vis.*, vol. 1, no. 4, pp. 321-331, 1988.

[3] S. M. Smith, “Fast robust automated brain extraction,” *Hum. Brain Mapp.*, vol. 17, no. 3, pp. 143-155, 2002.

[4] H. H. Chang, D. J. Valentino, G. R. Duckwiler, and A. W. Toga, “Segmentation of brain MR images using a charged fluid model,” *IEEE Transactions on Biomedical Engineering*, vol. 54, no. 10, October 2007.

[5] T. F. Chan and L. A. Vese, “Active contours without edges,” *IEEE Transactions on Image Processing*, Vol. 10, No. 2, February 2001.

[6] BrainWeb: Simulated Brain Database (SBD), http://brainweb.bic.mni.mcgill.ca/brainweb/

[7] Internet brain segmentation repository (IBSR), http://www.cma.mgh.harvard.edu/ibsr/

[8] H. H. Chang, A. H. Zhuang, D. J. Valentino, and W. C. Chu, “Performance measure characterization for evaluating neuroimage segmentation algorithms,” *NeuroImage*, vol. 47, no. 1, pp. 122-135, 2009.

Yu-Sheng Chen received his M.S. in 2013 from the Department of Engineering Science and Ocean Engineering at National Taiwan University, Taipei, Taiwan. He was formerly a graduate student in the Computational Biomedical Laboratory (CBEL) directed by Professor Herng-Hua Chang in the Department of Engineering Science and Ocean Engineering at National Taiwan University. His research interests include deformable models, image segmentation, and computational neuroscience.

Herng-Hua Chang received his Ph.D. in biomedical engineering in 2006 from the University of California at Los Angeles (UCLA). He was formerly a postdoctoral scholar with the Laboratory of Neuro Imaging (LONI) and a member of the Center for Computational Biology (CCB) at UCLA. Currently, he is an assistant professor of the Department of Engineering Science and Ocean Engineering at National Taiwan University, Taipei, Taiwan. Dr. Chang founded the Computational Biomedical Laboratory (CBEL), whose goal is to build computational bridges between engineering and medicine. His research interests include variational methods for image restoration, registration and segmentation, computational biology and radiology, biomechanics modeling and biosystem simulation, pattern analysis and computer graphics, as well as medical informatics for healthcare applications.